International Journal of Gas Turbine, Propulsion and Power Systems
June 2017, Volume 9, Number 2

Optimized Multidisciplinary Design of a Small Transonic Compressor for Active High-Lift Systems

Sönke Teichel[1], Tom Verstraete[2] and Jörg Seume[1]

[1]Institute of Turbomachinery and Fluid Dynamics, Leibniz Universität Hannover
Appelstr. 9, 30167 Hannover, Germany
[2]Turbomachinery & Propulsion Department, von Karman Institute for Fluid Dynamics
B1640 Rhode Saint Genese, Belgium

ABSTRACT

This paper presents the methodology and results of a design optimization of a single stage, axial compressor. At the design point, the compressor achieves a total pressure ratio of 2.33 at a mass-flow rate of 1.11 kg/s. The compressor is part of an electrically powered active high lift system (AHLS) for future civil aircraft. An automated process using numerical models to evaluate aerodynamic performances and mechanical loads due to centrifugal forces is used. This evaluation process is coupled to an evolutionary algorithm to help investigate the design-space. A parameterization strategy was developed to cover a wide design-space, excluding unreasonable designs. The goal was to satisfy the challenging design requirements of high pressure ratio, high power density and limited rotation speed imposed by the AHLS. The resulting design of a highly loaded compressor is characterized by significant end-wall slope and low blade aspect ratios, resembling a mixed flow compressor. According to CFD analysis it is predicted to cover the required operating points at total-total, polytropic efficiencies higher than 80 %.

INTRODUCTION

The process of designing turbomachinery combines different areas of mechanical engineering, e.g. aero design and structural design. The interactions between these different disciplines are complex and need to be considered in order to find a optimal solution that satisfies all design requirements. The investigation of the design-space to identify optimum designs, considering all relevant performance parameters, usually requires time consuming parameter studies and experience in the design process. To assist the multidisciplinary parametric studies, accelerating the design process, automated optimization is increasingly used ([1], [2], [3]). In this method, an optimization algorithm helps to investigate the parameterized design-space, aiming to satisfying the constraints and optimizing the objectives using an automated design and evaluation process. After determining the parameterization, the designer is then able to select the desired optimum design. In such design processes, the use of evolutionary algorithms is widely appreciated since these are able to find global optima over a wide range of parameters.

In this paper the optimization tool CADO (Computer Aided Design and Optimization Tool) [4] is used to design a small, single stage, transonic axial compressor with a maximum required total pressure ratio of 2.33 at a corrected mass-flow rate of 1.11 kg/s. The design process considers the aerodynamic design as well as the structural design using numerical simulation methods. A parameterization strategy based on fundamental compressor design methods is used, which allows the investigation of a wide design-space while minimizing the number of unreasonable designs evaluated during the optimization process. Using the developed process, the complete aerodynamic and structural design of the compressor blading can be performed with the assistance of an automated optimization process resulting in a single stage axial compressor with very high pressure ratios.

DESIGN PROCESS

The design process of turbomachinery is generally separated in different stages of complexity. In the so called preliminary design phase, the first major design decisions such as machine type and stage number are made using simplified physical models and empirical correlations. Based on these decisions, the final design parameters are fixed using detailed numerical design tools such as Computational Fluid Dynamics (CFD) and Computational Solid Mechanics (CSM).

Design Requirements

The investigated compressor is a key component of an active high-lift system which applies a combination of boundary layer suction and Coanda-Jet blowing. This research is part of the Collaborative Research Centre (in German: "Sonderforschungsbereich") SFB 880 [5] which is concerned with the fundamentals of efficient high lift for future civil aircraft.

One of the compressors is located in each flap of the wing, each powered by an electric motor to generate the suction and blowing mass-flow rate according to the current state of flight. The lift system is only in operation during take-off and landing, leading to a maximum operating time of about 4 min. The reference aircraft used to evaluate the technologies researched in the SFB 880 has six flaps per wing. While the five inner flaps only provide lift, the 6^{th} flap (aileron) also contributes to the maneuverability of the aircraft. In case of a rolling maneuver, additional jet momentum is required. These additional operating points with increased mass-flow rate and pressure ratio, and a confined radial space of about 0.3 m in the aileron flap amount to the most challenging compressor requirements of all flaps. For this reason these are the requirements used as a reference to design a suitable compressor system. The compressors required for the other flaps are less challenging concerning pressure ratio and may be deduced from the aileron system.

The required aileron compressor operating points resulting from reference aircraft design [5] are illustrated in Fig. 1. The considered states of flight are take-off, approach, and landing at altitudes of 0 m and 1500 m above sea level. At sea level, additionally to the international standard atmosphere (ISA) with $p_{\text{ref}} = 101325$ Pa and $T_{\text{ref}} = 288.15$ K, ambient temperatures of -40°C and 50°C are considered to represent the varying conditions experienced in aircraft application. The according ambient temperatures and pressures at 1500 m above sea level are determined using atmospheric models.

Manuscript Received on September 2, 2016
Review Completed on June 1, 2017

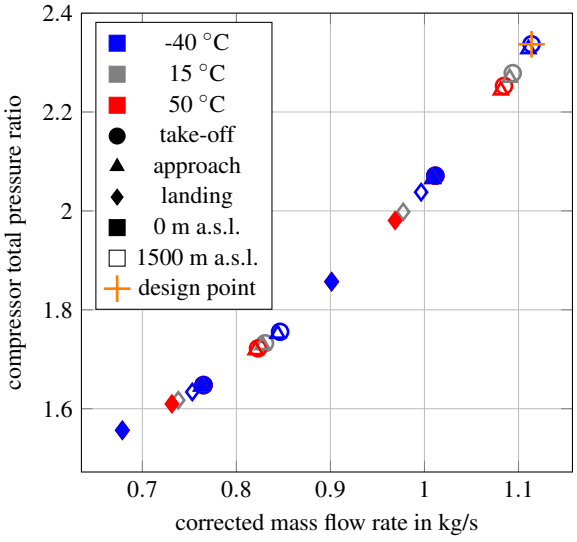

Fig.1: Required operating points of the aileron compressor.

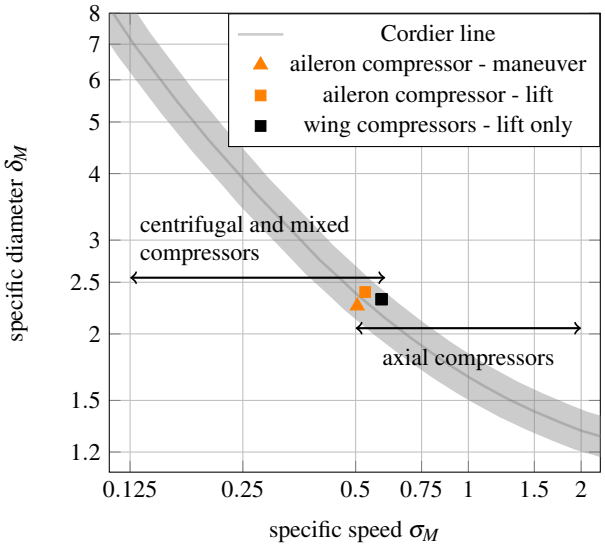

Fig.2: Cordier diagram for compressors with operating points [6]

At each of these states of flight, the compressor needs to be able to support both lift generation and additional maneuver support. To be able to compare these operating points, a corrected mass-flow rate ($\dot{m}_{\mathrm{corr}}$) is used which considers similarity of flow coefficient and Mach number with ISA as reference condition. In the results section a corrected rotational speed (n_{corr}) is used to consider similarity of the rotational Mach numbers.

$$\dot{m}_{\mathrm{corr}} = \dot{m} \cdot \frac{p_{\mathrm{ref}}}{p} \sqrt{\frac{T}{T_{\mathrm{ref}}}} \tag{1}$$

$$n_{\mathrm{corr}} = n \cdot \sqrt{\frac{T_{\mathrm{ref}}}{T}} \tag{2}$$

Correcting the mass-flow rate in this way leads to the compressor duty line illustrated in Fig. 1. At sea level the total pressure ratio and the corrected mass-flow rate remain unchanged with regard to ambient temperature since the ambient pressure remains the same. For these cases, Mach number and density variation balance out, leading to coinciding corrected operating points. At 1500 m above sea level not only ambient temperature but also the ambient pressure changes according to the standard atmospheric model occur. This leads to a shift of operating points towards higher total pressure ratios and higher corrected mass-flow rates with decreasing temperatures. The design point of the compressor is therefore chosen to be take-off at 1500 m above sea level with maneuver support at the equivalent ambient temperature of -40°C at sea level. This operating point requires the highest pressure ratio and largest flow rate and therefore determines the required machine size and required power. Aiming to maximize efficiency at this point will reduce the maximum power of the compressor and electric components leading to minimal system mass, which is critical for aircraft application.

An additional design feature to achieve high power density of the compressor system is the integration of the electric motor and the compressor on the same drive train. This way these components share the bearing system, making an additional gear box unnecessary. The design of the electrical components is done in a separate part of the project in close cooperation with the compressor design. For the expected compressor power of about 90 kW during operation, the achievable rotational speed was limited to 70,000 min^{-1} due to mechanical and thermal constraints in the electrical motor design.

Preliminary Design

To meet the requirements of the AHLS, both radial and axial compressors must be considered. Large turbocharger compressors meet the required corrected mass-flow range of 0.68 kg/s to 1.11 kg/s, these machines are usually meant to operate at higher total pressure ratios [7] and reach maximum efficiencies around 80 %. The capability of mixed-flow compressors of covering similar operating ranges as required in this project is demonstrated by [8]. In their work a mixed-flow compressor for corrected mass-flow rates of 0.4 kg/s to 1.5 kg/s and pressure ratios of up to 3 were achieved at max. total to total efficiencies of about 80 %. According to the authors, a recirculating bleed technique was required for this machine to achieve an acceptable operating range. Considering single stage axial compressors for this project the mass-flow rates are low and the total pressure ratio is very high compared to traditional machines. To minimize the mass and size of the system, multi stage compressors are not considered.

To select the appropriate compressor type and determine the major design parameters, dimensional analysis methods are applied. The Cordier diagram [6] gives a guideline in preliminary design on the basis of the non-dimensional parameters specific speed σ_M and specific diameter δ_M defined in:

$$\sigma_{\mathrm{M}} = \frac{n\sqrt{\dot{V}}}{|\Delta h_{\mathrm{tot,isen}}|^{3/4}} (2\pi^2)^{1/4} \tag{3}$$

$$\delta_{\mathrm{M}} = \frac{d_{\mathrm{max}} |\Delta h_{\mathrm{tot,isen}}|^{1/4}}{\sqrt{\dot{V}}} \left(\frac{\pi^2}{8}\right)^{1/4} \tag{4}$$

In Eqn. 3 and 4 the variable n represents the rotational speed, $\dot{V}$ the volumetric flow rate, $\Delta h_{\mathrm{tot,isen}}$ the isentropic enthalpy difference of the machine, and d_{max} the maximum machine diameter all in SI-Units. Based on existing, successful designs, empirical correlations, and simplified physical modeling, the so called Cordier diagram can be deduced. The resulting diagram for compressors is shown in Fig. 2. The Cordier line provides a relation between specific diameter and specific speed at which optimal efficiency of the compressor can be expected. Depending on the specific speed, the suitable machine type is indicated. The required operating points of the aileron compressor (Fig. 1) are indicated in Fig. 2 by the orange symbols, assuming a rotational speed of 70,000 min^{-1}, a maximum machine diameter of 130 mm, a flow coefficient ($\phi = \frac{c_{ax}}{u}$) of 0.45 and reaction of 0.6. Scaled correspondingly, the operating points of the other compressors for the inner flaps are indicated by the black symbol. It can be seen that the operating points of the compressors are located in a region where axial compressors and centrifugal / mixed compressors overlap. The operating points of the aileron compressor are leaning towards the centrifugal / mixed compressor while the operating points of the other compressors are leaning more towards the axial compressor region. Figure 3 shows a comparison of the operating ranges (indicated by the shaded areas) and expected efficiencies of axial- and centrifugal compressors adapted

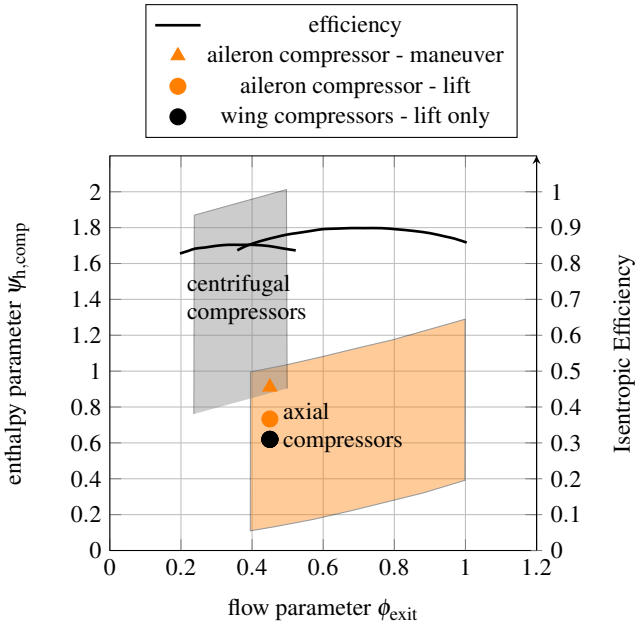

Fig.3: Typical compressor operating range and efficiency [6]

from [6]. Considering the enthalpy parameter ψ_{hcomp} and the flow parameter ϕ_{exit} (Eqn. 5 and 6) in Fig. 3, which relates static enthalpy increase and rotational speed of the machine, all operating points conform with typical axial compressor loading.

$$\psi_{hcomp} = \frac{2 \cdot \Delta h_{stat,comp}}{u_{exit}^2} \tag{5}$$

$$\phi_{exit} = \frac{c_m}{u_{exit}} \tag{6}$$

Considering the requirements of the compressor design emerging from the application as part of the AHLS, compactness, high power density, scalability of the compressor design for the inner flaps, and limited rotational speed are the most critical issues. The given mass-flow rates lead to comparable maximum rotor diameters of centrifugal and axial compressors for this application. Due to the radial diffuser and volute however, the radial space required for centrifugal compressors is significantly larger than for a comparable axial compressor, exceeding the available radial space in the wing of about 0.3 m. For the inner flaps higher mass-flow rates (up to 1.9 kg/s) and lower total pressure ratios (max. 1.85) are required. It is shown in Fig. 2 that for these machines, axial-flow compressors are the more suitable machine type. The better efficiencies of axial compressors in this region (Fig. 3) reduce the required power of the electrical components contributing to the advantage of axial-flow type compressors for this application considering compactness and high power density. Considering these system requirements, the concept of compact, single stage, transonic axial-flow-type compressors is pursued further for this compressor design.

Automated Detailed Design

In order to find an optimum design that satisfies the combined requirements of the active high lift system, a wide design-space needs to be investigated. This typically calls for the use of preliminary design tools which allow a rapid evaluation due to their limited level of resolved flow physics. However with the preliminary design method used, it was found that the reduced modeling approach resulted in unreliable prediction over the wide design-space considered for this type of compressor. To consider all significant aerodynamic effects in the design of this somewhat unusual axial compressor design, Computational Fluid Dynamics (CFD) were applied. An automated detailed design process was developed to be able to investigate a wide design-space with the assistance of an evolutionary optimization algorithm. Due to its qualities of convenient automation and parallelization, the CFD-software TRACE by DLR is used. For design purposes, the selected steady state, RANS (Reynolds Averaged Navier Stokes equation) model with the Shear Stress Transport (SST) turbulence model represent the significant aerodynamic effects adequately. The interface between rotating and stagnant domains is considered using the mixing plane approach. A structured computational grid of the compressor blade rows is generated automatically using DLR's grid generator G3DHexa. As part of the design process, a large number of CFD simulations need to be performed. It is therefore critical to reduce the computational effort by reducing the grid node numbers as much as possible, while still capturing all significant effects. Making use of the periodicity of the blading, only one rotor/stator passage is simulated. Grid sensitivity analysis showed that for the same number of nodes (approx. 0.6 million), a coarse grid which resolves the boundary layer with non-dimensional wall distances of $y^+ < 5$ using the low Reynolds modeling approach provides better representation of the flow than a grid with finer resolution of the passage flow but wall distances of $y^+ \approx 25$ and wall functions. For a better representation of boundary layer effects, the low Reynolds modeling approach was used. To ensure structural integrity of the blading, Computational Solid Mechanics (CSM) were applied to consider the significant centrifugal loads on the rotor blading. For this part of the design chain, the software CalculiX [10] was used. The structural mesh was generated as part of parameterized geometry generation provided by the optimization environment used. A subsequent, detailed mechanical analysis including vibration is done for the final design but is not part of the automated design process.

Optimization

The optimization environment used in this project is CADO (Computer Aided Design and Optimization Tool) [4]. It provides a parameterized turbomachine geometry generation tool using Bezier curves [3], a direct link for structural analysis using CalculiX, and a meta-model assisted, evolutionary optimization tool. As part of the parametrized geometry generation, a user defined number of Bezier control points can be applied to define the meridional shape and the blade shape. The blade is defined using spanwise and chordwise distributions of the blade angles, blade thickness, chord length, sweep, and lean. Based on this parameterized compressor geometry the degree of freedom of a compressor design can be selected according to the design task.

The optimization algorithm is based on the differential evolutionary algorithm [9] and allows constrained, multi-objective optimization. In this tool the disadvantage of evolutionary algorithms of requiring a large number of evaluations is managed by the use of a meta-model. Available meta models in this optimization environment are the Krigin-Model and Artificial Neural Networks [4]. These models can be included to interpolate the interactions between the design parameters on the basis of existing designs. Evaluating possible new designs with the meta-model first reduces the number of unreasonable designs evaluated with the computationally more expensive CFD and CSM, accelerating the process. To initialize a meta-model, an initial database of designs needs to be generated. For the meta model to accurately predict the performance of a design, all significant parameter interactions need to be represented by the underlying database. The size of the database is therefore depending on the number of optimization parameters n. Using Design of Experiments (DOE) methods the number of designs required to fully capture the relation between all n parameters by checking combinations of maximum and minimum values plus one central case is $2^n + 1$. The capabilities of evolutionary algorithms with well defined meta-models have been demonstrated over the last decade in many fields of turbomachinery design ([2], [3]). They are able to converge to optimal designs more directly with less computational effort than evolutionary algorithms without meta-model assistance. The use of

any meta-model however also introduces a possible cause for false optimization if the database of existing designs does not represent the design-space correctly. In this case a direct optimization without meta-model is often more reliable.

Parameterization

The selection of the degree of freedom (also called parameterization) is, together with the selection of the optimization objectives, one of the most critical steps when setting up an optimization process. Due to the unusual design requirements in this work, there is no existing compressor design which could serve as a basis to define the range of the design parameters. Instead a completely new compressor design needs to be found considering a wide design-space. To define the compressor design, the meridional flow path, hub and tip radii, rotational speed, blade number, chord length, blade angles, blade thickness distribution, as well as blade lean and sweep need to be determined for both blade rows. For an efficient optimization process the number of independent parameters is limited to approx. 30. Larger numbers of independent parameters would lead to excessive numbers of expensive CFD and CSM evaluations to be able to represent the interactions of the parameters correctly.
In order to obtain only reasonable compressor designs the design parameters cannot be varied independently of each other. The inlet blade angles for example are dependent on the inlet conditions, inlet area, and rotational speed of the machine. Considering basic compressor design parameters such as the flow coefficient, reasonable guess for many parameters can be defined. These fundamental compressor design methods can be used to reduce the number of optimization parameters without setting a large number of design parameters to be constant. The method used to define the rotor blade and flow passage during the optimization is illustrated in Fig. 4.
For the rotor design, specifying the design mass-flow rate ($\dot{m}$), inlet temperature (T_1), inlet pressure (p_1), circumferential Mach number (Ma_{tip}), flow coefficient (ϕ_{tip}), and inlet hub-to-tip ratio (ν_1) can be used to define the axial velocity (c_{ax}), the rotational speed (n), and the inlet tip and hub radii ($R_{\text{tip}_1}, R_{\text{hub}_1}$).

$$\dot{m} = \rho_{(T_1,p_1)} \cdot \left(\phi_{\text{tip}} \cdot Ma_{\text{tip}} \cdot a_{(T_1)}\right) \cdot \left(\pi \cdot R_{\text{tip},1}^2 \left(1-\nu_1^2\right)\right) \quad (7)$$

Specifying ranges for hub-to-tip ratios as well as tip radii factors at four axial positions, the meridional flow path is defined. Since the tip radius is allowed to increase, compressor designs with significant hub slope and low aspect ratios (span/chord) are possible. Varying hub-to-tip ratios allows to control the axial-flow velocity adjusting the area of the duct. From the values given for the compressor inlet, assuming no inlet swirl, reasonable guesses for the inlet blade angles can also be deduced (Eqn. 8-10). Based on these guesses the blade inlet angle is optimized to account for incidence and distortion of the inlet flow profile.

$$tan\left(\beta_{\text{in,tip}}\right) = \phi_{\text{tip}} = \frac{c_{\text{ax}}}{u_{\text{tip}}} \quad (8)$$

$$tan\left(\beta_{\text{in,midspan}}\right) = \frac{c_{\text{ax}}}{u_{\text{midspan}}} = \frac{c_{\text{ax}}}{2\pi R_{\text{midspan}} \cdot n} \quad (9)$$

$$tan\left(\beta_{\text{in,hub}}\right) = \frac{c_{\text{ax}}}{u_{\text{hub}}} = \frac{c_{\text{ax}}}{2\pi R_{\text{hub}} \cdot n} \quad (10)$$

Specifying blade deflection and blade camber at hub, mean and tip radius defines the camber line of the profiles. The chord lengths are scaled within a specified range. Thickness distributions are specified at hub and tip with a minimum leading edge thickness of 0.1 mm and a maximum blade thickness of 5 mm. The definition of blade sweep at hub and tip finalizes the blade definition. The solidity is varied to determine the blade number. The hub fillet radius is varied between 1 and 2 mm to find an optimum compromise with regards to the centrifugal stresses and aerodynamic performance. Hub fillets are therefore included in both the CFD and CSM simulations of each design. With the presented strategy, wide design

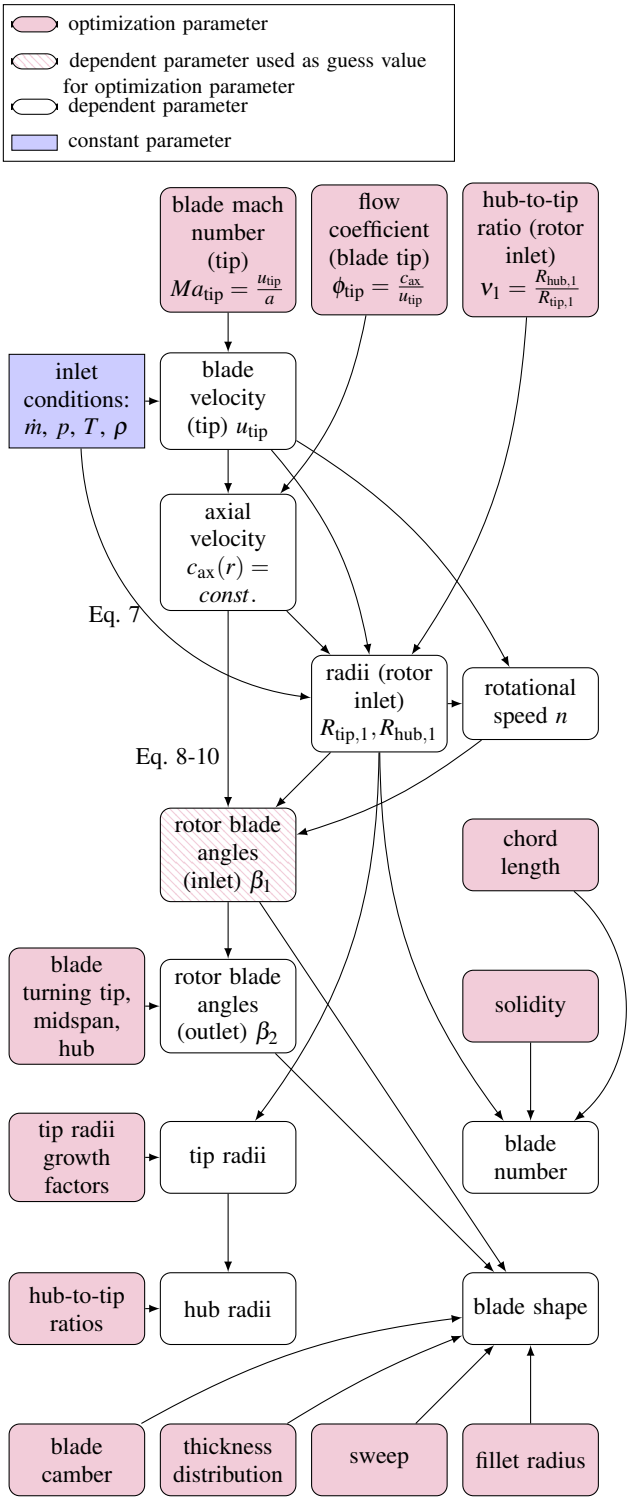

Fig.4: Parameterization strategy of the rotor and flow passage

space for the rotor blade row is achieved using 31 parameters.
To allow a sufficient degree of freedom the design of each blade row is done in separate steps. In the first step, the rotor optimization, the objectives are to obtain the required total pressure ratio at high total to total polytropic efficiency. As a third objective low rotational speed was introduced to take the limited speed of the motor which powers the compressor into account. The required total pressure ratio of the rotor accounts for the estimated 5% total pressure loss in the stator and is therefore higher than the design total pressure ratio of the stage. For the rotor optimization the described parameterization strategy (Fig. 4) is used. In the second step the

downstream stator is designed with the two objectives to obtain a high static pressure rise in the stator and a high total pressure ratio of the stage. The upstream rotor is simulated in every stator evaluation to consider rotor-stator-interaction. Since high pressure ratios for a given design mass-flow rate are desired, the operating point in the CFD simulation is fixed by specifying total inlet temperature and pressure, rotational speed and outlet mass-flow rate.

The stator design aims to recover the highest amount of static pressure from the total pressure at the rotor exit while at the same time causing the least total pressure loss. To account for rotor-stator interaction, the rotor exit blade angles are allowed to vary during the stator optimization. The parameterization of the stator blade row also allows full variability of the aerodynamic shape, including solidity, blade angles, blade camber, blade thickness distribution, chord length. Additionally, blade bow is allowed to shift aerodynamic loading to the midspan area of the stator with the goal to reduce end wall flow separation. Only the exit region of the meridional flow path is allowed to vary, in order to reduce stator loading by an increased radial shift of the flow path. The flow path is allowed to contract towards the exit to reduce swirl by increasing the axial velocity. Since many other machine parameters were fixed during the rotor design the stator is defined by 27 parameters. To avoid blade excitation, only stator blade numbers are allowed which have no common integer factor with the number of the upstream rotor blades.

A summary of the effective design parameters, objectives and constraints for rotor and stator optimization is given in Tab. 1. To limit the results of the optimization within the relevant range, constraints are imposed. For the rotor optimization only designs are considered which have a sufficiently high structural safety factor against centrifugal loads and which have high enough total pressure ratios. Designs with efficiencies of less than 75% at the design point are also excluded. Most importantly, designs with insufficient numerical convergence need to be excluded to base the optimization on reliable results.

RESULTS

In the following, the result of the optimized design process is presented. The the selection of the optimal blade row designs is explained and the resulting compressor stage is analyzed.

Table 1: Parameterization strategy of the compressor design.

rotor parameterization	
design parameters	rotational speed, meridional flow path, blade angles, blade camber, blade thickness distribution, chord length, blade number, blade sweep, hub fillet radius, total number: 31
objectives	high total polytropic efficiency design total pressure ratio ($\Pi_{tt} = 2.46$) low rotational speed
constraints	structural safety factor > 1.5 total pressure ratio > 1.8 total polytropic efficiency $> 75\%$ numerical convergence
stator parameterization	
design parameters	rotor exit angles, stator blade angles, blade camber, blade thickness distribution, chord length, blade lean, blade number, exit section of the meridional flow path, total number: 27
objectives	high stator static pressure ratio high stage total pressure ratio
constraints	static pressure ratio > 1.1 numerical convergence

Optimized Rotor Design

The first step of the optimized design process is the rotor design. With the given parametrization, a large variety of compressor designs is investigated. This challenges the automatic grid generation, as well as the default settings of the CFD solver to reach a sufficient level of convergence. For the rotor design, it was found that the meta-model was not able to reliably predict the compressor performance. For 31 parameters, the resulting number of evaluations exceeds the practical database size of about 1024 tests ($n = 10$) by several orders of magnitude. For design parameters with considerable dependence on each other, test numbers smaller than $2^n + 1$ often still lead to successful training of the meta model. However due to the reduction of dependent parameters using fundamental compressor design methods in the presented rotor parameterization, the dependence of the resulting parameters on each other is limited. The limited number of tests available to train the meta model together with a comparably high rate of failed evaluations results in an ill-trained meta-model with limited prediction quality. The rotor optimization was consequently done without a meta model, evaluating 10 individuals in each population.

The resulting pareto front from this optimization is shown in Fig. 5, it develops within the first 100 populations. Significant improvements concerning polytropic efficiency and total pressure ratio are achieved until population 140. Rotor designs with total pressure ratios between 1.8 and 2.65 were found to have efficiencies ranging from above 86 % to about 96 %. The optimal rotor design (marked with a pink triangle) is selected to match the target total pressure ratio, to achieve highest efficiency and to require low rotational speed which relieves the design requirements of the electrical motor. The corrected rotational speed of the Pareto optimal designs ranges from about 50,000 min^{-1} at low pressure ratios to about 70,000 min^{-1} for the highest pressure ratios. The selected design speed of the selected compressor is about 61,000 min^{-1} which together with a required power of about 65 kW still pushes the limits of current available technology of electrical machines.

Since a centrifugal stress analysis is part of the automated evaluation process, all compressor designs shown in Fig. 5 satisfy this structural constraint. The unstructured mesh with about 130,000 tetrahedral elements is generated for each blade passage design comprised of one blade and the corresponding blisk section. With increased element density in the blade and specifically the hub fillet region, the mesh sufficiently resolves the geometry. Compared to the CFD analysis the computational effort required for the additional stress analysis is not significant. Using a high-tensile alu-

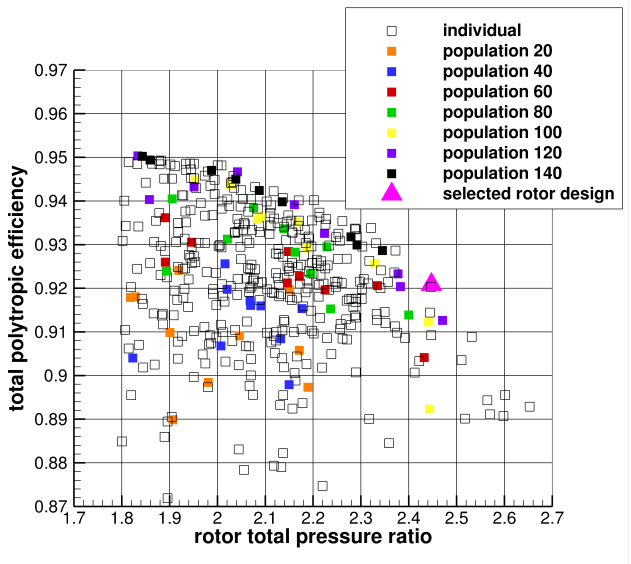

Fig.5: Resulting pareto front from rotor optimization

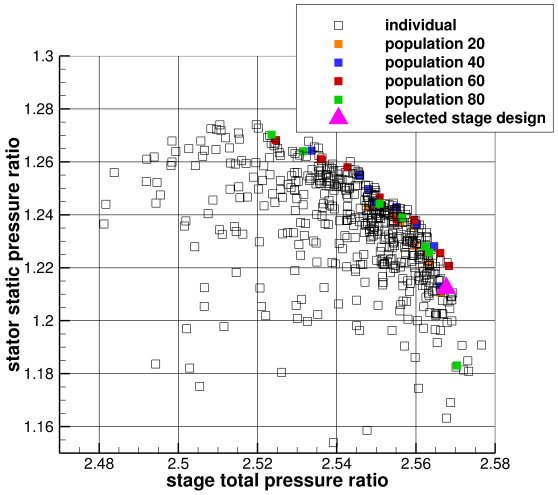

Fig.6: Resulting pareto front from stator optimization

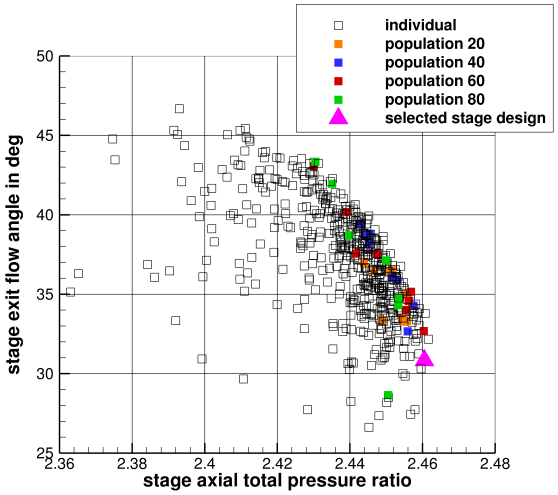

Fig.7: Results from stator optimization

minum alloy with a yield strength of approx. 390 MPa the overall safety factor of the selected optimal rotor at design speed is greater than 2.3.

Optimized Stator Design

For the following design step, a matching stator is designed for the selected rotor. To obtain high total pressure ratios, high velocities and large swirl are required at the rotor exit. Considering the mass-flow averaged values at the rotor exit plane, the flow exits with an absolute circumferential angle of about 65° with reference to the machine axis and an absolute Mach number of about 0.74. Given these inlet conditions, the purpose of the stator is to recover as much static pressure as possible. As part of the active high lift system, the compressor needs to supply the power for the Coanda blowing jet. In this regard, contrary to many other compressor applications, dynamic pressure is still a useful component of the flow for this application. A low exit swirl and a high fraction of static pressure at the stator exit is however desirable to reduce losses in the ducts connecting compressor and blowing slot. Since the supply of sufficient total pressure is critical, the stator needs to cause as little total pressure loss as possible.

The resulting optimization objectives used for the stator design are consequently high stator static to static pressure ratio and high stage total to total pressure ratio. The total pressure ratio of the stage is evaluated instead of stator total pressure loss to account for rotor-stator interaction. Due to the large number of optimization parameters and a comparably high rate of failed evaluations caused by the challenging stage aerodynamics, the stator optimization was also performed without meta-model assistance using the same settings as for the rotor optimization.

The designs resulting from the optimization are shown in Fig. 6 and Fig. 7. Stator static pressure ratios between 1.15 and 1.275 were obtained ranging in stage total pressure ratios between 2.48 and 2.58. Starting at low total pressure ratios both total and the static pressure rise can be increased. For total pressure ratios of the stage above 2.52 a further increase of total pressure ratio can only be obtained with a further decrease of stator static pressure ratio. Comparing the stage designs in Fig. 6 with the rotor designs in Fig. 5, it is noticeable that the stages obtain significantly higher total pressure ratios (see the "x-axis") than the rotor. The optimization of the meridional flow path and the exit blade angles of the rotor as part of the stator optimization obviously resulted in a further increase of the rotor's total pressure ratio. This gain in total pressure ratio exceeds the total pressure loss generated by the stator blade row. In Fig. 7 the same designs are shown with regards to the stage exit flow angle and the stage axial total pressure ratio. In can be seen that the stator designs have significant exit swirl ranging from 25° to about 47°. To exclude the undesirable swirl component of the stage exit total pressure, the stage axial total pressure ratio was defined (Eq. 11) which considers only the dynamic component at the stage exit directed in axial direction. This fraction is regarded as the usable total pressure in this application.

$$\Pi_{\mathrm{tt,ax}} = \frac{p_{\mathrm{tot,ax,out}}}{p_{\mathrm{tot,in}}} = \frac{p_{\mathrm{stat,out}} \cdot \left(1 + \frac{\gamma-1}{2} \cdot \left(\frac{c_{\mathrm{ax,out}}}{a}\right)^2\right)^{\frac{\gamma}{\gamma-1}}}{p_{\mathrm{tot,in}}} \tag{11}$$

Comparing Fig. 6 and Fig. 7, it can be seen that the axial total pressure ratio is about 0.11 lower than the actual total pressure ratio. Considering the comparably large exit swirl this difference is remarkably small. The kinetic energy contained by the exit swirl is consequently small compared the total energy of the exit flow. The selected stage design is marked by the pink triangle in Fig. 6 and Fig. 7. This design combines comparably low exit flow angles and high total pressure ratios. This design therefore provides the largest gain for the application in the active high lift system. Due to the large exit swirl and high velocity at stator inlet, high flow turning and increased stator static pressure rise do not coincide as it is usually observed in stator design. High flow turning for this design is only achievable through large flow separation in the stator. Although this dissipative turning does not cause significant total pressure loss it prevents significant stator static pressure rise. Unintuitively in this design, higher stator exit angles (less flow turning) lead to higher static pressure ratios.

Optimized Stage

Figure 8 shows the aerodynamic model of the resulting compressor stage. Major stage performance parameters at the design point are summarized in Tab. 2. As a result of the later presented CFD-generated performance map (Fig. 11) of the design it was necessary to shift the operating range by scaling the design to 95 % of the design mass-flow rate in order to better match the operating points of the AHLS. For this reason Fig. 9 shows the dimensions of the final, scaled design and not the optimized design. All other parameters in this section also correspond also to the scaled design. It can be seen that the compressor resembles a mixed compressor design due to its significant hub and shroud slope and the associated radius increase. The compressor blading has low aspect ratios below 0.3 and high solidities between 1.4 and 2.0 leading to narrow flow path comprised of short blades with high chord length. The rotor hub fillet radius is 2.5 mm. With the use of abrasive shroud coating it is assumed that a tip gap of 0.1 mm is achievable. In the stator row hub and shroud fillet radii are 2 mm. The conventional definitions of work and flow coefficient do not account for the significant radius

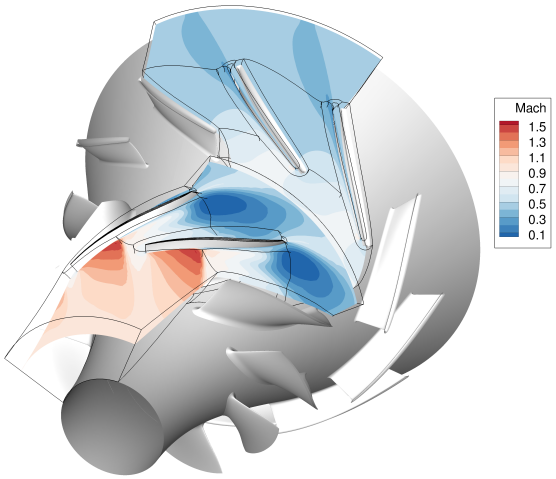

Fig.8: Aerodynamic compressor model of the optimized (non-scaled) design with flow solution at design point

increase of the rotor and therefore do not represent the compressor performance in a meaningful way. Considering the performance coefficients in Eqns. 5 and 6 it can be seen that the design exceeds the conventional operating range of axial compressors towards low flow ($\phi_{\text{exit}} = 0.33$) and high load ($\psi_{\text{h,comp}} = 0.86$). It is important to note that this definition of the compressor loading does not include the kinetic energy input to the flow and therefore under-represents the performance of this compressor. With a reaction of 0.77 the stator is less loaded than the rotor reducing flow separation in the stator. Considering the outer dimension of the compressor stage in Fig. 9, a compact design was achieved with a max. outer diameter of 194 mm and a length of 171 mm.

In Fig. 10, Mach contour plots of slices at constant spanwise positions in the hub, midspan and tip region of the compressor blading are shown, with the flow directed from left to right. It can be seen that a compression shock propagates over almost the whole span of the rotor blade row. The shock is located in the rotor passage propagating from the suction surface to the leading edge region of the neighbor blade. It is strongest in the tip region with relative Mach numbers of up to 1.4. Due to the shock, the flow decelerates within the full span to subsonic velocities. In the tip region towards the exit of the rotor, a large region with low relative velocities (Ma < 0.3) indicates an interaction of the passage flow and the tip leakage flow. The propagation of the low velocity region is limited to the upper blade span and therefore does not influence the machine

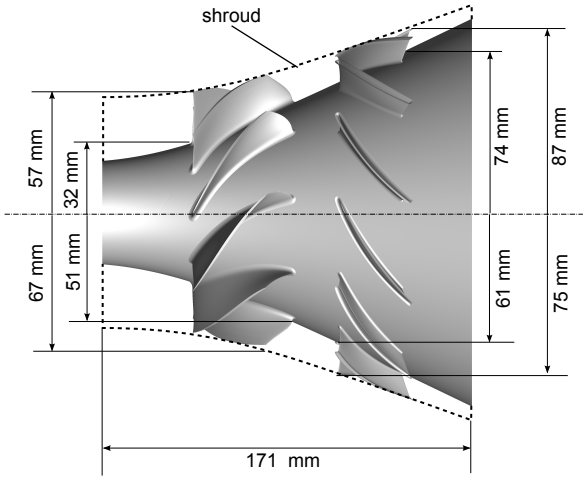

Fig.9: Final aerodynamic compressor model, scaled to better match operating range

performance significantly.

As discussed earlier, it can be seen in Fig. 10 that the flow turning in the stator is not sufficient to completely remove the swirl. The stator achieves a flow turning of about 37° leading to a stator exit flow an angle of about 31°. The flow is decelerated to an absolute Mach number of about 0.4. Low flow velocities in the hub region indicate flow separation in this area. Compared to previous designs, excessive flow separation at the stator blades and endwalls could be avoided due to the radial component and the contraction of the meridional flow path. Minimizing the tangential component of the stator exit flow is an important objective of this design task since this velocity component is expected to dissipate in the downstream diffuser and ducting leading to losses in these components. Despite the incomplete flow turning, this stator design provides the highest amount of useful energy to the active high lift system. The analysis of the axial total pressure ratio (Fig. 7) demonstrated sufficient usable total pressure ratio. Increased flow turning and static pressure rise would be desirable to make better use of the energy of the flow. But since for this application it is critical to reach a high total pressure ratio, the amount of swirl is accepted.

The CFD performance map of the stage is shown in Fig. 11. The performance data was obtained with the same numerical model as used in the optimization process but applying k-ω turbulence model instead of SST to avoid unphysical performance prediction in the high pressure, transonic region of the compressor map. To better match the operating points, however, it was necessary to scale the optimized design to 95 % of the design mass-flow rate to shift the operating range. The operating range of the compressor is sufficient to cover all required operating points. The maximum efficiencies around 90 % are obtained for operating points between 0.75 and 1 kg/s corrected mass-flow rate. The operating points with highest mass-flow are reached at lowest efficiency of around 80-85% due to the increasing shock losses..

Table 2: Compressor performance parameters at the design point.

stage	
corrected mass-flow rate	1.11 kg/s
total to total pressure ratio	2.33
total to total axial pressure ratio	2.22
total to static pressure ratio	2.00
polytropic efficiency	83.3 %
corrected rotational speed	60,125 min^{-1}
flow parameter	0.33
enthalpy parameter	0.86
reaction	0.77
rotor	
aspect ratio	0.3
chord length	62 mm
blade number	9
solidity	2.0
mean radius ratio	1.31
hub ramp angle	21.5°
shroud ramp angle	12.5°
stator	
aspect ratio	0.25
chord length	54 mm
blade number	11
solidity	1.4
mean radius ratio	1.19
hub ramp angle	25.3°
shroud ramp angle	19.3°
pressure coefficient	0.4
loss coefficient	0.14

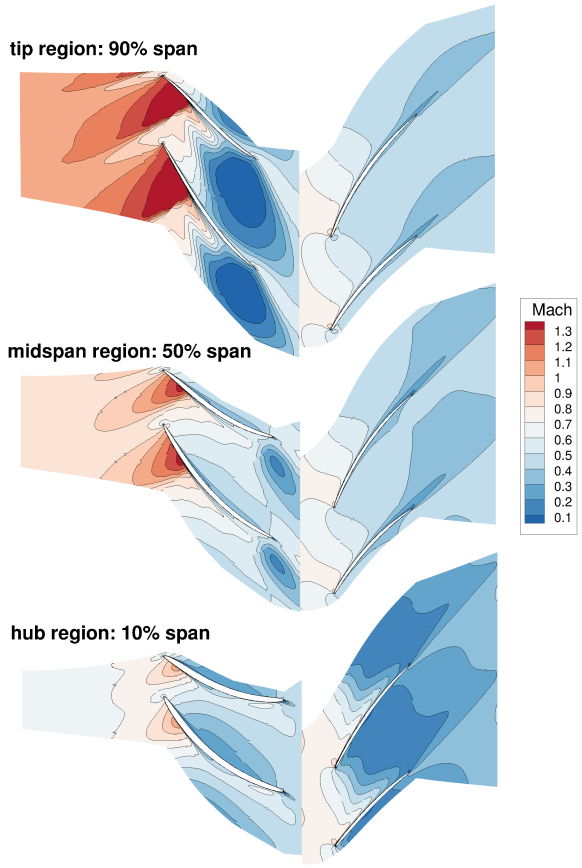

Fig.10: Mach number contour plots of compressor at design point at hub, midspan, and tip region.

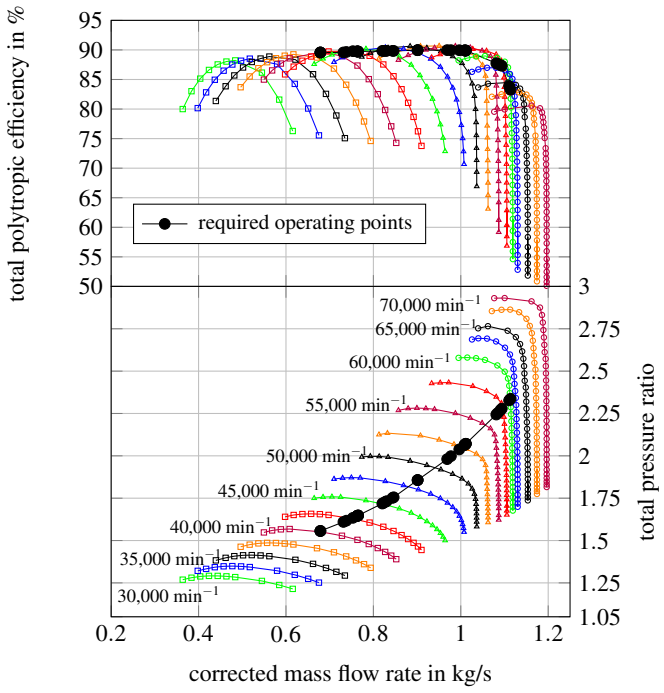

Fig.11: CFD performance map of the compressor design with required operating points using the $k-\omega$ turbulence model.

CONCLUSIONS

The optimized design process of a compact, highly loaded single stage axial compressor for an active high-lift system for aircraft was presented and the resulting design discussed. Established dimensional analysis methods motivated the decision for an axial-flow type compressor for this design task. A parameterization strategy was developed to cover a wide compressor design-space in the detailed design phase.

The variability of the designs is currently limited by the reliability of the evaluation process, in particular the quality of the numerical convergence. This limitation is not only caused by the limited mesh quality of some individuals, but also by the challenging aerodynamics of the designs.

According to CFD analysis, the resulting compressor stage is able to reach the required total pressure ratios of up to 2.33 and covers the required operating points at low mass-flow rate with efficiencies higher than 83 % and rotational speed of less than 65,000 min^{-1}, well below the speed limit of the electric motor powering the compressor. For the selected design the compressor efficiency drops to 80 % for mass-flow rates higher than 1.0 kg/s.

The resulting compressor design exceeds the common design space of compressors towards low flow parameters of 0.33 and high enthalpy parameters of 0.86. The design has a significant radial component resembling mixed-flow type compressors. Future experimental validation will be done to determine the performance of the design and to asses the validity of the numerical model used.

ACKNOWLEDGMENTS

The authors would like to thank the German Research Foundation (DFG) for supporting this fundamental research in active high-lift systems for future aircraft as part of the Collaborate Research Centre 880 (SFB 880).

References

[1] Büche, D., Guidati, G., Stoll, P., 2003. "Automated Design Optimization of Compressor Blades for Stationary, Large-Scale Turbomachinery", *Proceedings of: ASME Turbo Expo 2003*, doi:10.1115/GT2003-38421

[2] Ellbrant, L., 2014. "Multi-objective CFD-based design method for axial compressors", *Doctoral thesis, Chalmers University of Technology Goteborg, Sweden*

[3] Joly, M.M., 2014. "Multifidelity, Multidisciplinary Optimization of Turbomachines with Shock Interaction.", *Doctoral thesis, Texas ASM University, USA*

[4] Verstraete, T. 2010. "CADO: a Computer Aided Design and Optimization Tool for Turbomachinery Applications", *2nd International Conference on Engineering Optimization*, Lisbon, Portugal

[5] Radespiel, R., Heinze, W., 2014. "SFB 880: fundamentals of high lift for future commercial aircraft.", *CEAS Aeronautical Journal* 5, 239251. doi:10.1007/s13272-014-0103-6

[6] Dubbel, H., Grote, K.-H., Feldhusen, J., 2011. "Dubbel: Taschenbuch fr den Maschinenbau", *Springer*, Berlin.

[7] Garrett by Honeywell - Turbocharger, URL: `http://www.turbobygarrett.com/turbobygarrett/turbocharger#GT6041`, accessed 05/12/2015.

[8] Hazby, H., Casey, M., Numakura, R., Tamaki, H., 2014. "A Transonic Mixed-flow Compressor for an Extreme Duty", *ASME Turbo Expo 2014: Turbine Technical Conference and Exposition. American Society of Mechanical Engineers*

[9] Storn, R., Price, K., 1997. "Differential evolutiona simple and efficient heuristic for global optimization over continuous spaces", *Journal of global optimization* 11, 341359.

[10] Dhondt, G.D.C., 2004. "The finite element method for three-dimensional thermomechanical applications", *Wiley*, Hoboken